Principal Deformations Modes of Articulated Models for the Analysis of 3D Spine Deformities

Jonathan Boisvert, Farida Cheriet, Xavier Pennec, Hubert Labelle, Nicholas Ayache

Electronic Letters on Computer Vision and Image Analysis 7(4):13-31, 2008

Principal Deformations Modes of Articulated Models for the Analysis of 3D Spine Deformities

Jonathan Boisvert[*+−], Farida Cheriet[*−], Xavier Pennec[+], Hubert Labelle[−] and Nicholas Ayache[+]

[*] *École Polytechnique de Montréal, P.O. Box 6079, Suc. Centre-Ville, H3C 3A7, Montréal, Canada*
[+] *Asclepios Project Team, INRIA, 2004 route des Lucioles - BP 93 06902 Sophia Antipolis Cedex, France*
[−] *Sainte-Justine Hospital, 3175, Chemin de la Côte-Ste-Catherine, Montréal, Canada*

Received 9th May 2008; accepted 4th December 2008

Abstract

Articulated models are commonly used for recognition tasks in robotics and in gait analysis, but can also be extremely useful to develop analytical methods targeting spinal deformities studies. The three-dimensional analysis of these deformities is critical since they are complex and not restricted to a given plane. Thus, they cannot be assessed as a two-dimensional phenomenon. However, analyzing large databases of 3D spine models is a difficult and time-consuming task. In this context, a method that automatically extracts the most important deformation modes from sets of articulated spine models is proposed.

The spine was modeled with two levels of details. In the first level, the global shape of the spine was expressed using a set of rigid transformations that superpose local coordinates systems of neighboring vertebrae. In the second level, anatomical landmarks measured with respect to a vertebra's local coordinate system were used to quantify vertebra shape. These articulated spine models do not naturally belong to a vector space because of the vertebral rotations. The Fréchet mean, which is a generalization of the conventional mean to Riemannian manifolds, was thus used to compute the mean spine shape. Moreover, a generalized covariance computed in the tangent space of the Fréchet mean was used to construct a statistical shape model of the scoliotic spine. The principal deformation modes were then extracted by performing a principal component analysis (PCA) on the generalized covariance matrix.

The principal deformations modes were computed for a large database of untreated scoliotic patients. The obtained results indicate that combining rotation, translation and local vertebra shape into a unified framework leads to an effective and meaningful analysis method for articulated anatomical structures. The computed deformation modes also revealed clinically relevant information. For instance, the first mode of deformation is associated with patients' growth, the second is a double thoraco-lumbar curve and the third is a thoracic curve. Other experiments were performed on patients classified by orthopedists with respect to a widely used two-dimensional surgical planning system (the Lenke classification) and patterns relevant to the definition of a new three-dimensional classification were identified. Finally, relationships between local vertebrae shapes and global spine shape (such as vertebra wedging) were demonstrated using a sample of 3D spine reconstructions with 14 anatomical landmarks per vertebra.

Key Words: Shape Analysis, Articulated Models, Spinal Deformities, Scoliosis, 3D Reconstruction, Surgical Classifications.

Correspondence to: <jonathan.boisvert@polymtl.ca>

Recommended for acceptance by Francisco Perales
ELCVIA ISSN:1577-5097
Published by Computer Vision Center / Universitat Autònoma de Barcelona, Barcelona, Spain

1 Introduction

Articulated models are collections of objects linked together so that the relative motion of any two parts is rigid (combination of a 3D rotation and a translation). This family of models can be used to describe a wide variety of objects. A popular application is human gait analysis from video sequences. In this type of application, human body motion is characterized by articulations states and about thirty degrees of freedom are usually necessary to obtain convincing results. This number of degrees of freedom (DOF) makes model estimation from video sequences challenging from a computational perspective. However, probabilistic methods can be used to discard unlikely positions and to deal with occlusions [7, 14, 28, 33].

The human body being composed of 206 bones, it is easily understandable that those models are highly simplified representations of the human skeleton. Only articulations critical to gait description are considered and only these articulations' most important DOF are included in the models. Thus, subtle pathological motions could be inadvertently discarded. For example, most articulated models used for motion capture only attribute one degree of freedom to the knee, whereas many musculoskeletal problems of the knee are characterized by more complex 3D rotations.

This situation contrasts with statistical shapes models currently used to process radiological spine images. Those statistical models are based on point-to-point correspondences [20, 3] and many points are sampled on each vertebra, therefore the number of DOF could reach several hundreds. These statistical shape models describe efficiently the local shape of the vertebrae and they can improve the performances of segmentation and registration algorithms. However, they fail to take into account that the spine is a collection of vertebrae linked together by soft tissues (discs, muscles, ligaments, *etc.*). Capturing the articulated nature of the spine will lead to a statistical shape model that can be interpreted more intuitively and that will uncover more clinically relevant relationships.

Point-to-point correspondences are therefore not the best choice of primitives. A more natural choice would be to use frames (points associated with three orthogonal axes) to deal with articulated anatomical structures. The main reason for this choice is that frames enable a more natural analysis of the relative orientations and positions of the models, whereas point primitives would only properly deal with positions. In this context, articulated models of the spine will be created by associating a frame to each vertebra. The deformations of the spine shape will then be described in terms of rigid transformations applied to those frames.

A variability model of inter-vertebral rigid transformations based on Lie group properties was recently proposed [5]. However, the inter-vertebral transformations were analyzed individually thus discarding the coupling between different vertebral levels. It is difficult to take into account the coupling between all vertebral levels because of the high dimensionality of the model. In fact, there are 5 lumbar and 12 thoracic vertebrae (excluding cervical vertebrae) and a rigid transformation has 6 DOF, which means that an articulated description of the spine shape is characterized by at least 102 DOF. A clinician can hardly perform the analysis of such large variability model. It is therefore necessary to find a way to extract only the most meaningful modes of variability. These modes will indicate what varies the most from a geometric perspective in a given group, thus helping the physician in the task of analyzing large sets of 3D spine models, which is a necessary but tedious task to define a clinically relevant 3D classification.

In this context, the main contributions of this paper are to propose a method based on Riemannian geometry to perform principal components analysis on articulated spine models and to apply that method to a large database of scoliotic patients in order to construct the first statistical atlas of 3D deformation patterns for adolescent idiopathic scoliosis (a pathology that causes spine deformations). The combination of point-based and frame-based model will also be demonstrated to analyze the relation between the shape of the spine and the shape of individual vertebrae.

The remaining of the manuscript is divided in four sections. The next section review relevant works performed about scoliosis deformities analysis and about dimensionality reduction applied to articulated models. Section 3 then presents the proposed methods and the acquisition materials used for this study. The results obtained on large databases of scoliotic patients are presented in Section 4. Finally, Section 5 summarizes the

conclusions and new perspectives that resulted from this study.

2 Background

2.1 3D Spine Models Classifications

Analyzing large databases of 3D spine models is becoming more and more important because there is a consensus among orthopedic surgeons that spinal deformations such as adolescent idiopathic scoliosis (AIS) are three-dimensional. However, there is no consensus yet regarding how to use 3D information to improve patients' care.

Classification is a decisive part of AIS patient assessment because it is used in the preoperative planning of corrective surgeries. King first proposed a classification of frontal thoracic curves, which was used to guide surgeries performed with the Harrington instrumentation [16]. This classification did not address sagittal deformations neither lumbar curves. Moreover, its reliability was contested [17, 31]. Lenke later proposed another classification [18] that includes lumbar and sagittal modifiers. Lenke classification is more complete; however combining 2D measures is different from performing a real 3D analysis. Thus, new three-dimensional classifications of the spinal deformations associated with AIS are being investigated.

However, taking into account the three-dimensional nature of the deformations is far from being trivial. Many classifications were recently introduced. Duong et al. [8] used a wavelet transform of the vertebrae centroids and a clustering method to agglomerate similar 3D spine shapes. The method is technically elegant but its complexity might not be compatible with clinical practice. Poncet et al. [27] proposed a classification that is based solely on spine torsion. Spine torsion is certainly an important factor to take into account but Duong et al. demonstrated that it is not the only one. Finally, Negrini et al. [23, 22, 21] recently proposed a classification based on "quasi-3D" indices (measure performed on multiple 2D projections). The main drawbacks of their approach are the *ad hoc* character of the indices selected and the two-dimensional nature of the classification.

In summary, analyzing large databases of 3D spine models is an important task but it is also a difficult and time-consuming one. Automatically extracting the most important deformation modes from a set of articulated spine models would greatly help surgeons to reliably and efficiently explore 3D spine models databases, which is a necessary prerequisite to the definition of a clinically relevant 3D classification of scoliotic deformities.

2.2 Principal components analysis of the 3D articulated spine models

Dimensionality reduction applied to the spine or to articulated models is not a new idea and methods were proposed in the past. As a part of a method that aim to predict the geometry of the spine based on the geometry of the trunk, Bergeron et al. [4] performed a principal component analysis on the 3D coordinates of vertebrae centers in the frequency domain. The most important limitation of this approach is that vertebrae orientations are not modeled. Moreover, performing the analysis in the frequency domain does not allow a physically grounded intuitive interpretation of the results. Benameur et al. [3] and Fleute et al. [10] both proposed principal components analysis (PCA) based spine registration method but only the shapes of the vertebrae were considered not the global spine shape.

Principal components analysis was also used to process articulated body models. Yacoob and Black [32] applied PCA analysis on motion parameters measured with respect to the image plane in the context of activity recognition. Unfortunately, since the measurements are not intrinsic to the geometry of the articulated object the same viewpoint and camera have to be used, which is unrealistic for clinical studies that involves multiple research centers. Gonzalez et al. [12] and Green et al. [13] both performed a PCA analysis on aligned time-series of articulated models descriptions in order to recognize human actions. Jiang and Motai [15] proposed a similar approach for on-line robot learning. Finally, Al-Zubi and Sommer [1] performed PCA to learn articulated motions of human arms. These approaches used representations that were either only based on 3D coordinates or only based on an angular description of the articulated body. However, using both positions and orientations

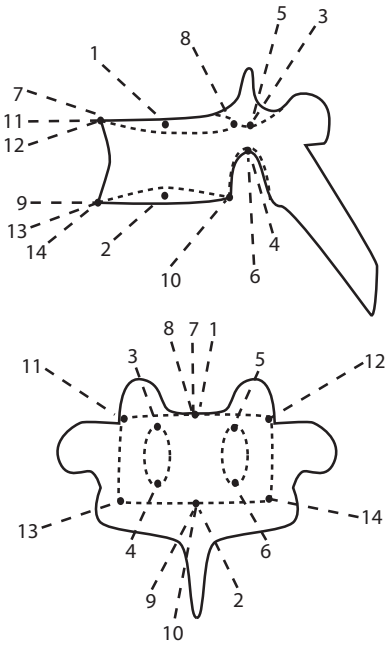

Figure 1: Anatomical landmarks used to digitize the spine geometry and to analyze local vertebra shape. Top: lateral view. Bottom: posterior view.

would allow a better separation of different physiological phenomena such as pathological deformations and normal growth (that is expected to be dominated by translation). Moreover, these methods compute the mean without taking into account that 3D rotations form a curved manifold. Therefore, the obtained results depend on the arbitrary configuration of the local coordinates systems used to perform angular measurements.

3 Material and Methods

This section is divided in three subsections. One of the problems with previous attempts to find variability modes from 3D spine models was that their underlying spine geometry representations were based on point-to-point correspondences, which are not adapted to an analysis of orientations. The first subsection (3.1) will thus present an articulated description of the human spine that includes both vertebrae's relative position and orientation as well as the method used to estimate these articulated spine models from radiographs.

The chosen articulated description uses rigid transformations to encode the relative position and orientation of the vertebrae. However, rigid transformations naturally belong to a Lie group and conventional statistical methods usually apply only in vector spaces. To alleviate this problem, the second subsection (3.2) will present how to rigorously generalize concepts such as the mean and the covariance to articulated spine models.

Finally, the last subsection (3.3) will introduce a simple mechanism to extract and visualize the most significant deformations modes observed in a database of articulated spine models.

3.1 Articulated Spine Models from Radiographs

Articulated models could be estimated from a wide variety of image modalities. Computed tomography or magnetic resonance could be used since the images recorded using those modalities are three-dimensional. However, large portions of the spine deformations are lost when patients are asked to lie down. Moreover, adolescent idiopathic scoliosis patients often present postural problems, which are relevant to the analysis. In

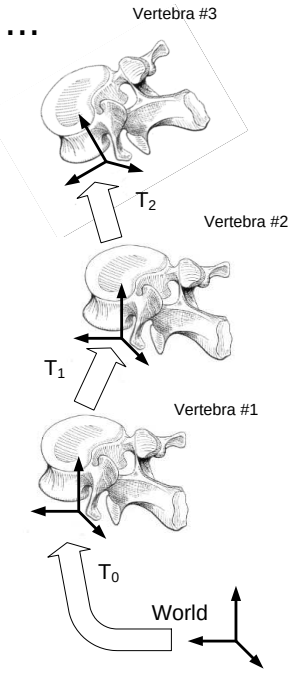

Figure 2: Frames and transformations used to express the spine as an articulated model.

light of those constraints, we choose to use multi-planar radiography in order to digitize the 3D anatomy of the patients' spine.

Multi-planar radiography is a simple technique where two (or more) calibrated radiographs of a patient are taken to compute the 3D position of anatomical landmarks using a triangulation algorithm. It is one of the few imaging modalities that can be used to infer the three-dimensional anatomy of the spine when the patient is standing up. Furthermore, bi-planar radiography of scoliotic patients is routinely performed at Sainte-Justine hospital (Montreal, Canada).

The anatomical landmarks used in this study are illustrated in Figure 1. The identification of all anatomical landmarks is time consuming and costly because it is performed by a qualified technician. However, it provides a more robust anatomical matching of landmarks, which ensures a more precise 3D reconstruction. Thus, only the anatomical landmarks 1 to 6 were used when only the shape of the spine and not the local shapes of the vertebrae was analyzed. These anatomical landmarks were identified on each vertebra from T1 (first thoracic vertebra) to L5 (last lumbar vertebra) on a posterior-anterior and a lateral radiograph. The 3D coordinates of the landmarks were then computed and the deformation of a high-resolution template using dual kriging yielded a total of 24 reconstructed landmarks. The accuracy of this method was previously established to 2.6 mm [2].

Once the anatomical landmarks presented in Figure 1 are reconstructed in 3D, they are expressed in the local coordinates system of their respective vertebra (see Stokes [29] for a formal definition of the local coordinates system of a vertebrae). These local landmarks coordinates $p_1, p_2, \ldots, p_n$ (where n is the number of anatomical landmarks used for each vertebra) will be used to analyze the vertebrae shapes. Each vertebra is then rigidly registered to its first upper neighbor and the resulting rigid transformations are recorded. By doing so, the spine is represented by a set of rigid transformations (see the Figure 2). These inter-vertebral transformations $T_1, T_2, \ldots, T_{17}$ will be used to analyze the spine shape.

The combination of the local landmarks coordinates and the inter-vertebral transformations is especially well adapted to an analysis of the spinal deformities since the inter-vertebral rigid transformations describe the state of the physical links that alter the shape of the whole spine while the local landmarks coordinates can quantify the local vertebral deformations.

Most scoliotic patients are adolescents or pre-adolescents and the spine length of these patients varies considerably. At this point one might be tempted to normalize the spine models to improve comparability. However,

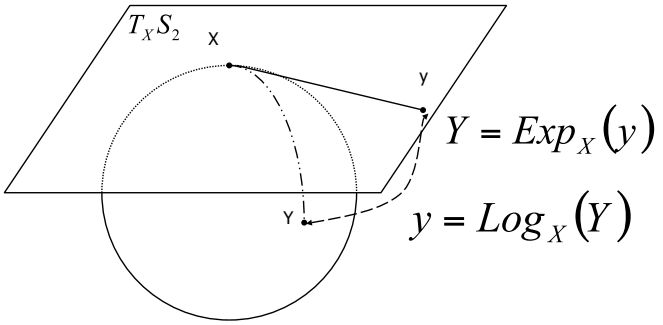

Figure 3: Graphical representation of the Log_X and Exp_X maps on a three-dimensional sphere.

the development of many musculoskeletal pathologies, such as adolescent idiopathic scoliosis, is tightly linked with the patient growth process. Thus, normalization could discard valuable information and should be avoided in most applications.

3.2 Elements of Articulated Models Statistics

The articulated spine models presented in the last subsection express the spine shape using a vector of inter-vertebral rigid transformations. This idea is very intuitive and models closely the pathological progression mechanisms of spinal deformities. However, rigid transformations do not naturally belong to a vector space (they belong to a curved Riemannian manifold) and simple operations necessary to conventional multi-variate analysis such as addition and scalar multiplication are not defined on those. A generalization of concepts as simple as the mean and the covariance is therefore needed.

One could be tempted to parameterize the rigid transformations using one of the many available representations (Euler angles and translation vector, for example) and then to compute the mean and covariance on that representation. However, the result would not be intrinsic. In other words, the mean and covariance would be dependent on the viewpoint from which the orientation and position would have been measured.

The distance is a general concept that can be used to perform those generalizations and Riemannian geometry offers a mathematical framework to work with primitives when only a distance is available. Concepts of probability and statistics applied to Riemannian manifolds were recently studied [26]. Moreover, a Riemannian framework was also used in the context of statistical shape modeling to perform PGA (principal geodesic analysis) on medial axis representations [9].

3.2.1 Exponential and Logarithmic Maps

In a complete Riemannian manifold $\mathcal{M}$ the shortest smooth curve $\gamma(t)$ such that $\gamma(0) = x$ and $\gamma(1) = y$ (with $x, y \in \mathcal{M}$) is called a geodesic and the length of that curve is the distance between x and y. Two important maps can be defined from the geodesics: the exponential map Exp_x which maps a vector ∂_x of the tangent plane $T_x\mathcal{M}$ to the element reached in a unit time by the geodesic that starts at x with an initial tangent vector ∂_x and the logarithmic map Log_x which is the inverse function of Exp_x. In other words, these two maps enable us to "unfold" the manifold on the tangent plane (which is a vector space) and to project an element of the tangent plane to the manifold (see Figure 3 for an example of Log_x and Exp_x).

In this paper, the spine shape is modeled as a set of frames associated to local coordinates systems of vertebrae. The modifications of the spine geometry are then modeled as rigid transformations applied to those frames. In order to compute the principal deformations modes (from equation 7), the exponential and logarithmic maps associated with a distance function on rigid transformations are thus needed.

A rigid transformation is the combination of a rotation and a translation. Defining a suitable distance on the translational part is not difficult since 3D translations belong to a real vector space. However, the choice of a

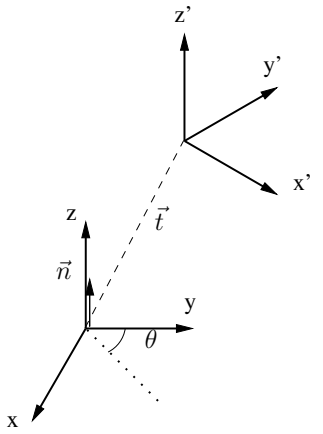

Figure 4: Rigid transformation expressed by an axis of rotation n, an angle of rotation θ and a translation vector t

distance function between rotations is more complex. Rotations are usually expressed using a three by three matrix that belongs to the special orthogonal group $\mathcal{SO}^3$ and simple solutions, like the norm of the difference, does not respect the prerequisites conditions for distance functions.

To define a suitable distance between rigid transformations, another representation of the rotations called the rotation vector is needed. This representation is based on the fact that a 3D rotation can be fully described by an axis of rotation supported by a unit vector n and an angle of rotation θ (see figure 4). The rotation vector r is then defined as the product of n and θ.

The conversion from the rotation vector to the rotation matrix is performed using the Rodrigues rotation equation (see [11] for details):

$$R = I + \sin(\theta)S(n) + (1 - \cos(\theta))S(n)^2 \quad \text{with} \quad S(n) = \begin{bmatrix} 0 & -n_z & n_y \\ n_z & 0 & -n_x \\ -n_y & n_x & 0 \end{bmatrix}$$

And the inverse map (from a rotation matrix to a rotation vector) is given by the following equations:

$$\theta = \arccos(\frac{Tr(R) - 1}{2}) \quad \text{and} \quad S(n) = \frac{R - R^T}{2\sin(\theta)} \tag{1}$$

Using the rotation vector representation, a left-invariant distance ($d(T_3 \circ T_1, T_3 \circ T_2) = d(T_1, T_2)$) between two rigid transformations can easily be defined:

$$d(T_1, T_2) = N_\omega(T_2^{-1} \circ T_1) \quad \text{with} \quad N_\omega(T)^2 = N_\omega(\{r, t\})^2 = \|\omega r\|^2 + \|t\|^2 \tag{2}$$

Where ω is used to weight the relative effect of rotation and translation, r is the rotation vector and t the translation vector. Because the selected distance function is left-invariant, we have $\text{Exp}_\mu(x) = \mu \circ \text{Exp}_{Id}(D(\mu)^{-1}x)$ and $\text{Log}_\mu(T) = D(\mu)\text{Log}_{Id}(\mu^{-1} \circ T)$ with $D(x) = \frac{\partial}{\partial y} x \circ y|_{y=Id}$. Furthermore, it can be demonstrated that the exponential and log map associated with the distance of equation 2 are the mappings (up to a scale) between the combination of the translation vector and rotation vector and the combination of the rotation matrix and the translation vector [25].

$$\text{Exp}_{Id}(T) = \begin{vmatrix} R(r) \\ t \end{vmatrix} \quad \text{and} \quad \text{Log}_{Id}(T) = \begin{vmatrix} \omega r(R) \\ t \end{vmatrix}$$

The Riemannian structure of the anatomical landmarks used to quantify the local shape of the vertebrae is much more simple. In fact, anatomical landmarks simply belong to $\Re^3$, which is a vector space. Thus, with

respect to the Euclidian distance, the anatomical landmarks belong to a flat Riemannian manifold. The Exp and Log maps are then as simple as translations of the original landmarks:

$$\text{Exp}_p(q) = p + q \quad \text{and} \quad \text{Log}_p(r) = r - p \quad \text{with} \quad p, q, r \in \Re^3$$

3.2.2 Fréchet Mean

For a given distance, the generalization of the usual mean can be obtained by defining the mean as the element μ of a manifold $\mathcal{M}$ that minimizes the sum of the distances with a set of elements $x_{0...N}$ of the same manifold $\mathcal{M}$:

$$\mu = \arg\min_{x \in \mathcal{M}} \sum_{i=0}^{N} d(x, x_i)^2$$

This generalization of the mean is called the Fréchet mean. Since it is defined using a minimization, it is difficult to compute it directly from the definition. However, it can be computed using a gradient descent performed on the summation. The following iterative equation summarizes this operation:

$$\mu_{n+1} = \text{Exp}_{\mu_n}(\frac{1}{N} \sum_{i=0}^{N} \text{Log}_{\mu_n}(x_i)) \tag{3}$$

3.2.3 Generalized Covariance

The variance (as it is usually defined on real vector spaces) is the expectation of the L_2 norm of the difference between the mean and the measures. An intuitive generalization of the variance on Riemannian manifolds is thus given by the expectation of a squared distance:

$$\sigma^2 = \frac{1}{N} \sum_{i=0}^{N} d(\mu, x_i)^2 \tag{4}$$

To create statistical shape models it is necessary to have a directional dispersion measure since the anatomical variability of the spine is anisotropic [5]. The covariance is usually defined as the expectation of the matricial product of the vectors from the mean to the elements on which the covariance is computed. Thus, a similar definition for Riemannian manifolds would be to compute the expectation in the tangent plane of the mean using the log map:

$$\Sigma = \frac{1}{N} \sum_{i=0}^{N} \text{Log}_{\mu}(x) \text{Log}_{\mu}(x)^T \tag{5}$$

3.2.4 Multivariate Case

The Fréchet mean and the generalized covariance make it possible to study the centrality and dispersion of one primitive belonging to a Riemannian manifold. However, to build complete statistical shape models, it would be most desirable to study multiple primitives altogether. Therefore, a generalized cross-covariance Σ_{fg} is needed.

$$\Sigma_{fg} = \frac{1}{N} \sum_{i=0}^{N} \text{Log}_{\mu_f}(f_i) \text{Log}_{\mu_g}(g_i)^T$$

A natural extension is to create a multivariate vector $f = [f_1, f_2, f_3, \ldots, f_k]^T$ where each element corresponds to a part of a model made of several primitives. In our case, these primitives are the inter-vertebral rigid transformations and the local anatomical landmarks described in Figure 1. The mean and the covariance of this multivariate vector will thus be:

$$\mu = \begin{bmatrix} \mu_1 \\ \mu_2 \\ \vdots \\ \mu_k \end{bmatrix} \quad \text{and} \quad \Sigma = \begin{bmatrix} \Sigma_{f_1 f_1} & \Sigma_{f_1 f_2} & \cdots & \Sigma_{f_1 f_k} \\ \Sigma_{f_2 f_1} & \Sigma_{f_2 f_2} & \cdots & \Sigma_{f_2 f_k} \\ \vdots & \vdots & & \vdots \\ \Sigma_{f_k f_1} & \Sigma_{f_k f_2} & \cdots & \Sigma_{f_k f_k} \end{bmatrix} \tag{6}$$

This is very similar to the conventional multivariate mean and covariance except that the Fréchet mean and the generalized cross-covariance are used in the computations.

3.3 Principal Deformations

The equation 6 allows us to compute a statistical shape model for a group of models made of several primitives. However, the different primitives will most likely be correlated which makes the variability analysis very difficult. Furthermore, the dimensionality of the model is also a concern and we would like to select only a few important uncorrelated components.

Unlike the manifold itself, the tangent plane is a vector space and its basis could be changed using a simple linear transformation. Thus, we seek an orthonormal matrix A ($AA^T = I$) to linearly transform the tangent plane ($\text{Log}_\mu(g) = A\text{Log}_\mu(f)$) such as the generalized covariance in the transformed tangent space is a diagonal matrix ($\Sigma_{gg} = \text{diag}\,(\lambda_1, \lambda_2, \ldots, \lambda_k)$). The covariance matrices of the transformed tangent space and of the original tangent space are connected by the following equation:

$$\Sigma_{gg} = \text{diag}\,(\lambda_1, \lambda_2, \ldots, \lambda_k) = A\Sigma_{ff}A^T$$

If A is rewritten as $A = [a_1, a_2, \ldots, a_k]^T$, then it is easy to show that:

$$[\lambda_1 a_1, \lambda_2 a_2, \ldots, \lambda_k a_k] = [\Sigma_{ff} a_1, \Sigma_{ff} a_2, \ldots, \Sigma_{ff} a_k] \tag{7}$$

The line vectors of the matrix A are therefore the eigenvectors of the original covariance matrix and the elements of the covariance matrix in the transformed space are the eigenvalues of the original covariance. This is the exact same procedure that is used to perform PCA in real vector spaces. Like for real vector spaces, the variance is left unchanged since $\sigma^2 = \text{Tr}(\Sigma_{ff}) = \text{Tr}(\Sigma_{gg})$ and the cumulative fraction of the variance explained by the first n components is:

$$p = \frac{1}{\sigma^2} \sum_{i=1\ldots n} \lambda_i$$

A shape model can be re-created from coordinates of the transformed tangent space simply by going back to the original tangent space and projecting the model on the manifold using the exponential map. So if α_i is the coordinate associated with the i^{th} principal component, the following equation can be used to re-create a shape model:

$$S = \text{Exp}_\mu(\sum_{i=1}^{k} \alpha_i a_i)$$

4 Results and Discussion

This section presents and discusses the results obtained using the method previously described. Principal spine deformations modes are presented in three different contexts. First of all, the principal spine deformation modes of a group of patients afflicted by AIS is presented. These results indicated that the principal deformation modes can efficiently extract the most important modes of variability and that those modes have a strong clinical meaning. Then, a comparison of the principal deformations modes of two groups of scoliotic patients classified according to the Lenke classification [18] is introduced. This experiment demonstrates that the principal deformation modes can extract clinically relevant patterns that could easily be missed by a direct visualization of the spine models. Finally, we present results obtained from a group of spine models with 14 landmarks by vertebra where we show that global deformations of the spine are correlated with vertebral deformations.

4.1 Spine Shape Analysis

The method described in the previous sections was applied to a group of 307 scoliotic patients. The patients selected for this study had not been treated with any kind of orthopedic treatment when the radiographs were taken. Therefore, the inter-patients variability observed was mainly caused by anatomical differences and not by any treatment. A total of 6 anatomical landmarks were identified manually by a qualified technician, this number of landmarks is sufficient to analyze the shape of the spine, but is not enough to properly analyze vertebrae shapes. Thus, only the inter-vertebral rigid transformations were used for this experiment.

The only additional parameter that needs to be selected is ω, which balances the relative importance of the translation and rotation (see Equation 2). In some applications, rotations are more important than translations (or the converse) and this parameter may be used to bias the results toward the most important part of the rigid transformations. In our case, however, we did not want to introduce such bias. Thus, ω was selected so that the rotations and the translations had the same contribution to the global variance. This criteria lead to a numerical value of $\omega = 20$.

To illustrate the different deformation modes retrieved using the proposed method, four models were reconstructed for each of the first five principal deformation modes. Those models were reconstructed by setting α_k to $-3\sqrt{\lambda_k}$, $-\sqrt{\lambda_k}$, $\sqrt{\lambda_k}$ and $3\sqrt{\lambda_k}$ for $k = 1 \ldots 5$ while all others components (α_i with $i \neq k$) were set to zero (see figures 5 and 6). In theory, a total of 102 principal deformation modes could be extracted. However, 102 figures would certainly overload this paper. The first five modes (in term of variance explained) illustrate well the power of the proposed method since they can be understood without an extensive medical background. The interpretation of less important deformations modes is subtler. Furthermore, the 3D spine models in our databases are corrupted by a certain amount of acquisition noise. Thus, principal deformations modes associated with small variances are more likely to be dominated by noise.

A visual inspection revealed that the first five principal deformation modes have clinical meanings. The first mode is associated with the patient growth because it is mainly characterized by an elongation of the spine and also includes a mild thoracic curve. The second principal deformation mode could be described as a double thoraco-lumbar curve, because there are two curves: one in the thoracic segment (upper spine) and another in the lumbar segment (lower spine). The third principal mode of deformation is a simple thoracic curve (the apex of the curve is in the thoracic spine), but it is longer than the thoracic curve observed in the first principal component. It is also interesting to note that, in addition to the curves visible on the posterior-anterior view, the second and third principal deformation modes are also associated with the development of a kyphosis (back hump) on the lateral view. The fourth component is a lumbar lordosis (lateral curve of the lumbar spine). Finally, the fifth component is related to the patient's frontal balance.

Those curve patterns are routinely used in different clinical classifications of scoliosis (used to plan surgeries). For instance, the reconstructions built from the first principal deformation mode would be classified using King's classification [16] as a type II or III (depending on which reconstruction is evaluated), the second

deformation mode would be associated to King's type I or III and the third principal deformation could be associated to King's type IV.

Previously those patterns were derived from surgeons' intuition using 2D images and clinical indices, whereas it is now possible to automatically compute those patterns from statistics based only on 3D geometries.

Furthermore, the cumulative variance explained by an increasing number of principal deformations modes (illustrated in Figure 7) shows the capacity of the proposed method to reduce the number of dimensions of the model while keeping a large part of the original variance. This property could be used in registration or reconstruction algorithms. Also, since about 50 % of the variance is explained by the first five principal deformations modes, it appears that a careful analysis of more principal deformation modes by trained medical experts might reveal more clinically pertinent knowledge in the future.

The variability observed from our dataset is predominantly associated with anatomical variability, but it also includes variability caused by other factors such as patients' postures and landmark reconstruction errors. Therefore, the principal deformations modes associated with small eigenvalues are likely to be more closely related to acquisition noise than to anatomical variations between individuals.

4.2 Surgical Classifications Analysis

Classifications of spinal deformities are used for several purposes : as a training tool for new residents, as mean of communication between practitioners, as a guideline for the selection of a corrective treatment, *etc*. Current classifications used for adolescent idiopathic scoliosis are based on 2D measures performed on radiographs. However, the deformities are three-dimensional and therefore it is very likely that clinically relevant sub-groups could be identified by a 3D analysis.

Two groups of untreated AIS patients with two different curve types (according to the Lenke classification [18]) were identified from the Sainte-Justine Hospital's archive: 86 patients with type I curves and 47 patients with type V curves. Type I curves are characterized by a main thoracic curve while type V curves are thoracolumbar or lumbar curves. A qualified physician performed the classification and six anatomical landmarks were identified on each radiograph. Only the inter-vertebral rigid transformations were used to compute the principal deformation modes (not the anatomical landmarks). The first three principal modes of deformations (with $\omega = 20$) computed from the two groups of patients are presented in Figure 8 and Figure 9.

Figure 8 shows that the most important mode of deformation for scoliotic spines of type I is an elongation of the spine combined with the development of a right thoracic curve and little curvature modification visible from the lateral view. Type I curves are defined as main thoracic curvatures and right curves are more prevalent then the left among scoliotic patients. Moreover, smaller patients are usually younger and scoliosis progress during growth. Thus, this deformation mode is compatible with the progression of the disease for patient that suffers from a curve of the first type. The second mode of deformation is associated with a double curve and strong sagittal curvature of the lower spine (lordosis) caused largely by a rotation of L5 (the lowest lumbar vertebra). This L5 rotation could indicate a deformation of a structure below the spine, thus it would be very interesting to also analyze the position and orientation of the pelvis. Finally, the third mode exhibit the development of a right thoracic curve, but a curve with a lower apex (close to T9-T10) than the right thoracic curve present in the first deformation mode.

The deformations modes presented in Figure 9 were computed in the database of scoliotic models with curves of the fifth type. The first mode of deformation in this case is characterized by an elongation of the spine associated with the creation of a left thoracolumbar curve. Lenke defined curves of the fifth type as thoracolumbar or lumbar curves. This first deformation mode is therefore similar to the first deformation mode of type 1 curves as they both depict the worsening of the 2D curve they were aimed to represent and are combined with an elongation of the spine. The second mode of deformation is thoracolumbar curve going from left to right with an increasing kyphosis. Finally, the third mode is the transformation of a double curve with very little lordosis and kyphosis to a small thoracolumbar curve with large lordosis and kyphosis.

These two figures indicate that the principal deformations modes can efficiently capture the clinically in-

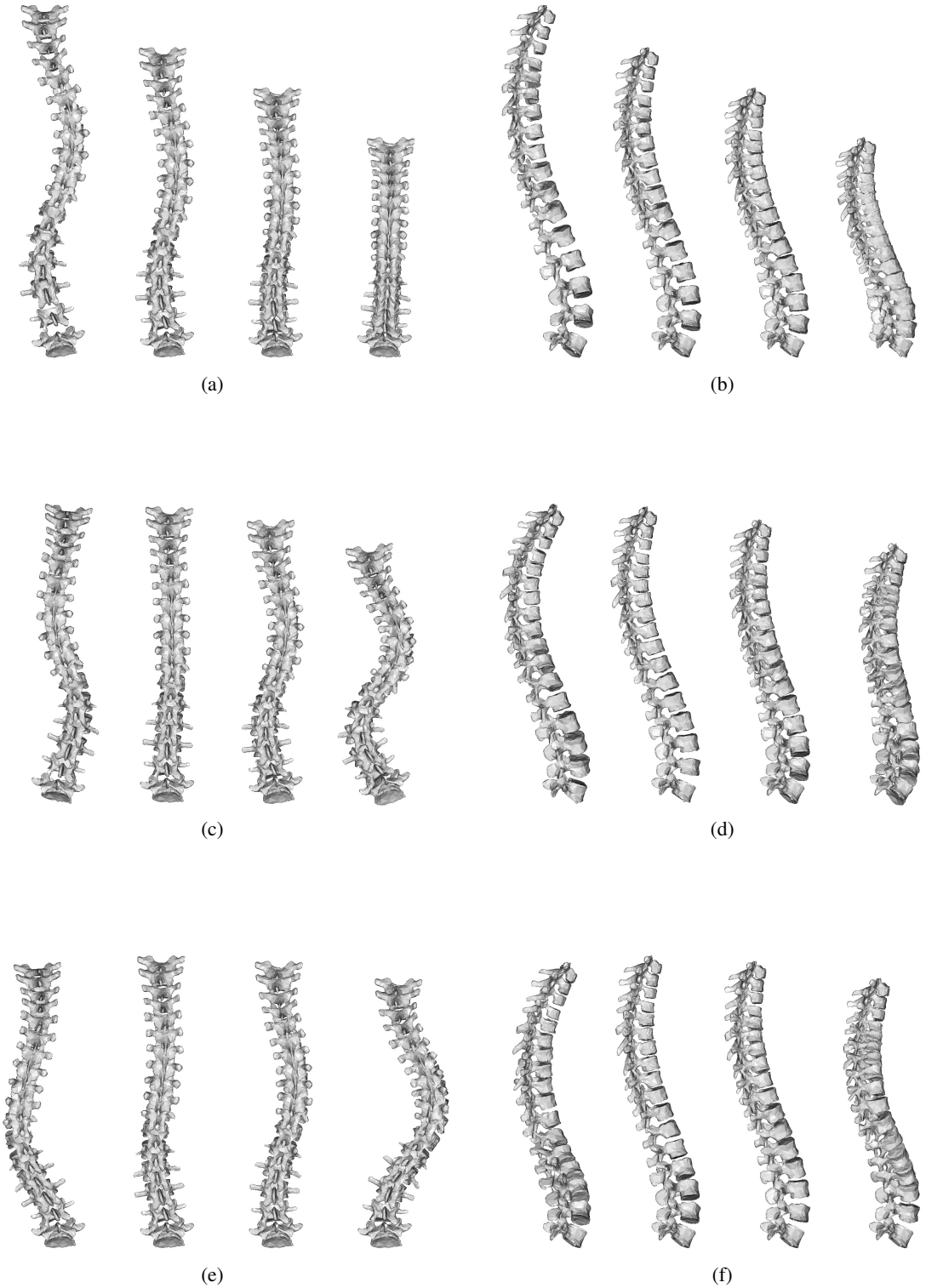

Figure 5: First, second and third principal deformation modes of an AIS patient database. Posterior-anterior view (a) and lateral view (b) of the first principal deformation mode. Posterior-anterior view (c) and lateral view (d) of the second principal deformation mode. Posterior-anterior view (e) and lateral view (f) of the third principal deformation mode. Spine models were rendered for -3, -1, 1 and 3 times the standard deviation explained by the corresponding deformation mode.

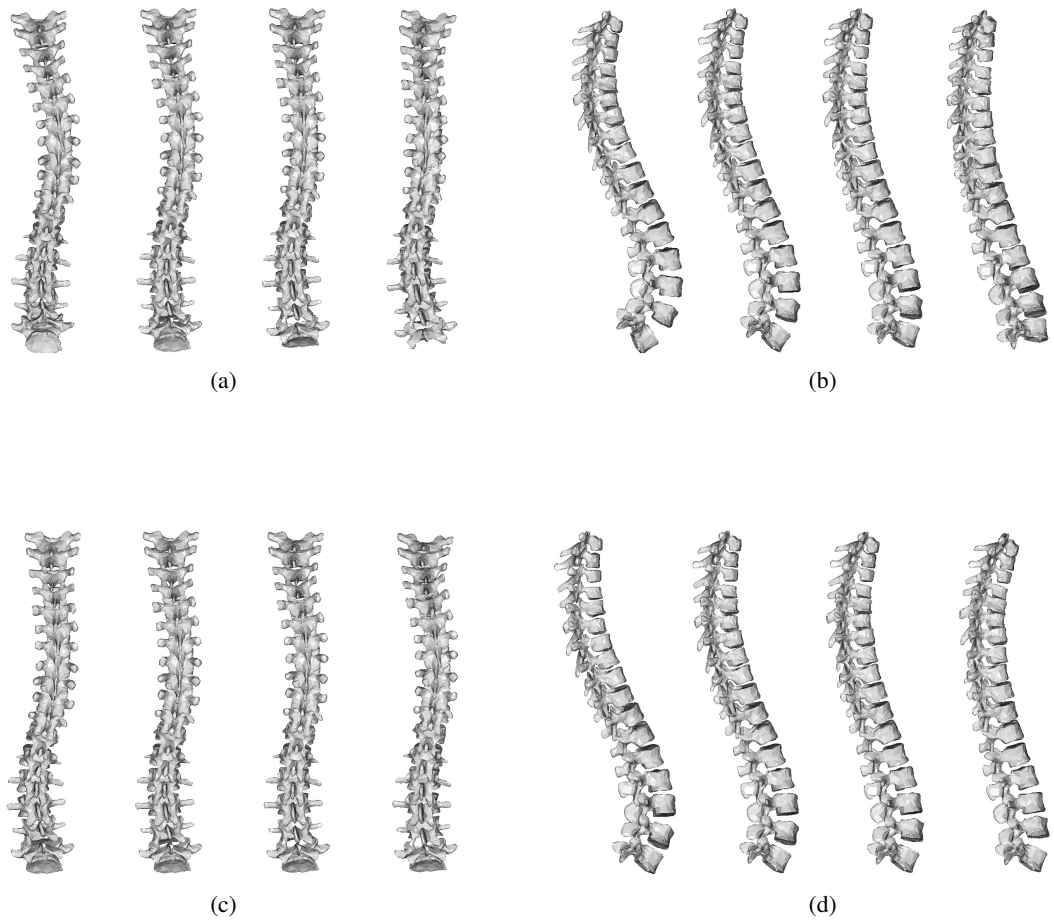

Figure 6: Fourth and fifth principal deformation modes of an AIS patient database. Posterior-anterior view (a) and lateral view (b) of the fourth principal deformation mode. Posterior-anterior view (c) and lateral view (d) of the fifth principal deformation mode. Spine models were rendered for -3, -1, 1 and 3 times the standard deviation explained by the corresponding deformation mode.

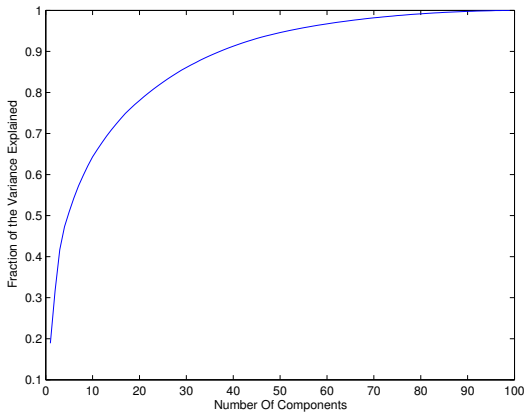

Figure 7: Fraction of the variance explained by the principal deformation modes

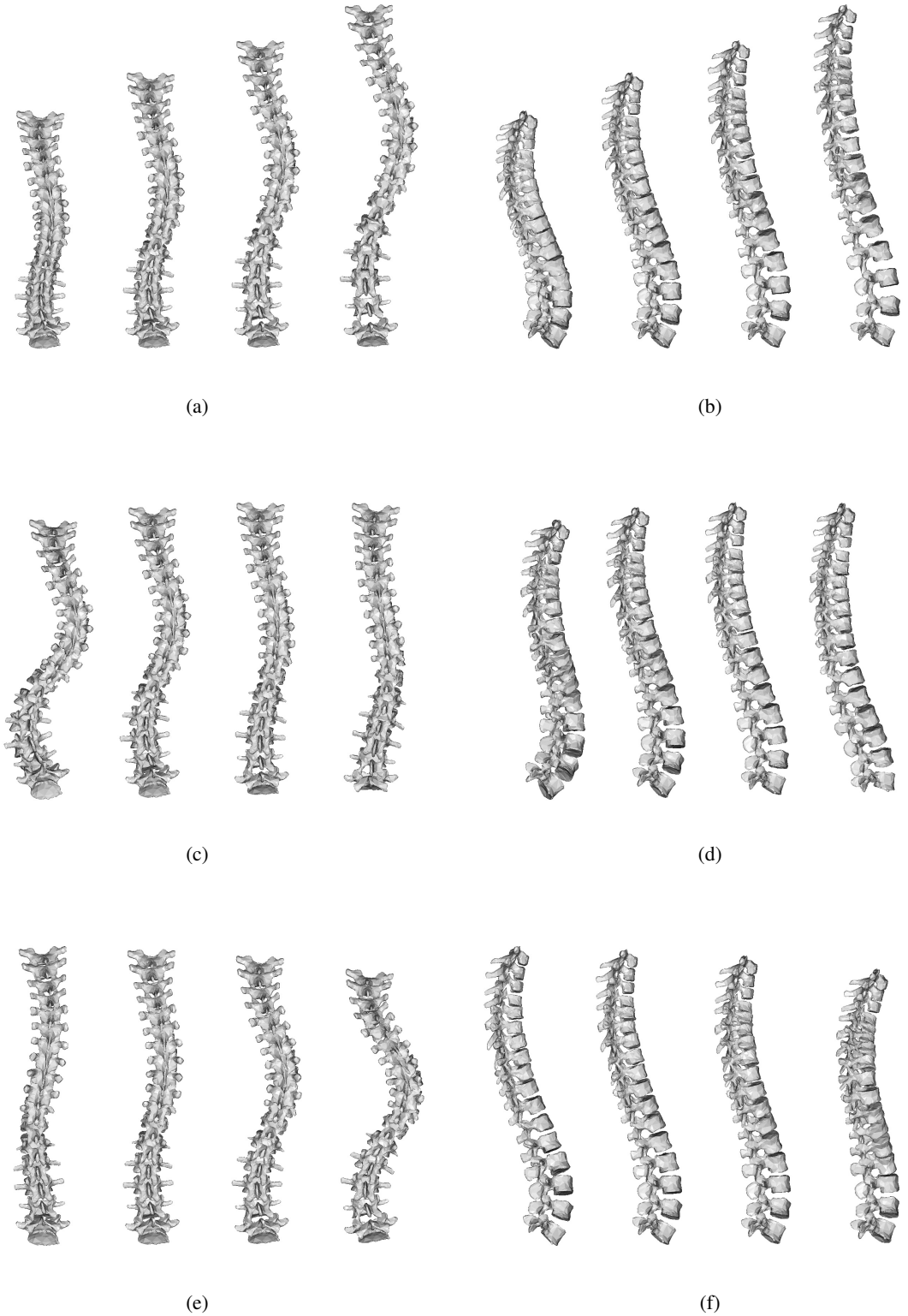

Figure 8: First, second and third principal deformation modes of AIS patient with type I curves. Posterior-anterior view (a) and lateral view (b) of the first principal deformation mode. Posterior-anterior view (c) and lateral view (d) of the second principal deformation mode. Posterior-anterior view (e) and lateral view (f) of the third principal deformation mode. Spine models were rendered for -3, -1, 1 and 3 times the standard deviation explained by the corresponding deformation mode.

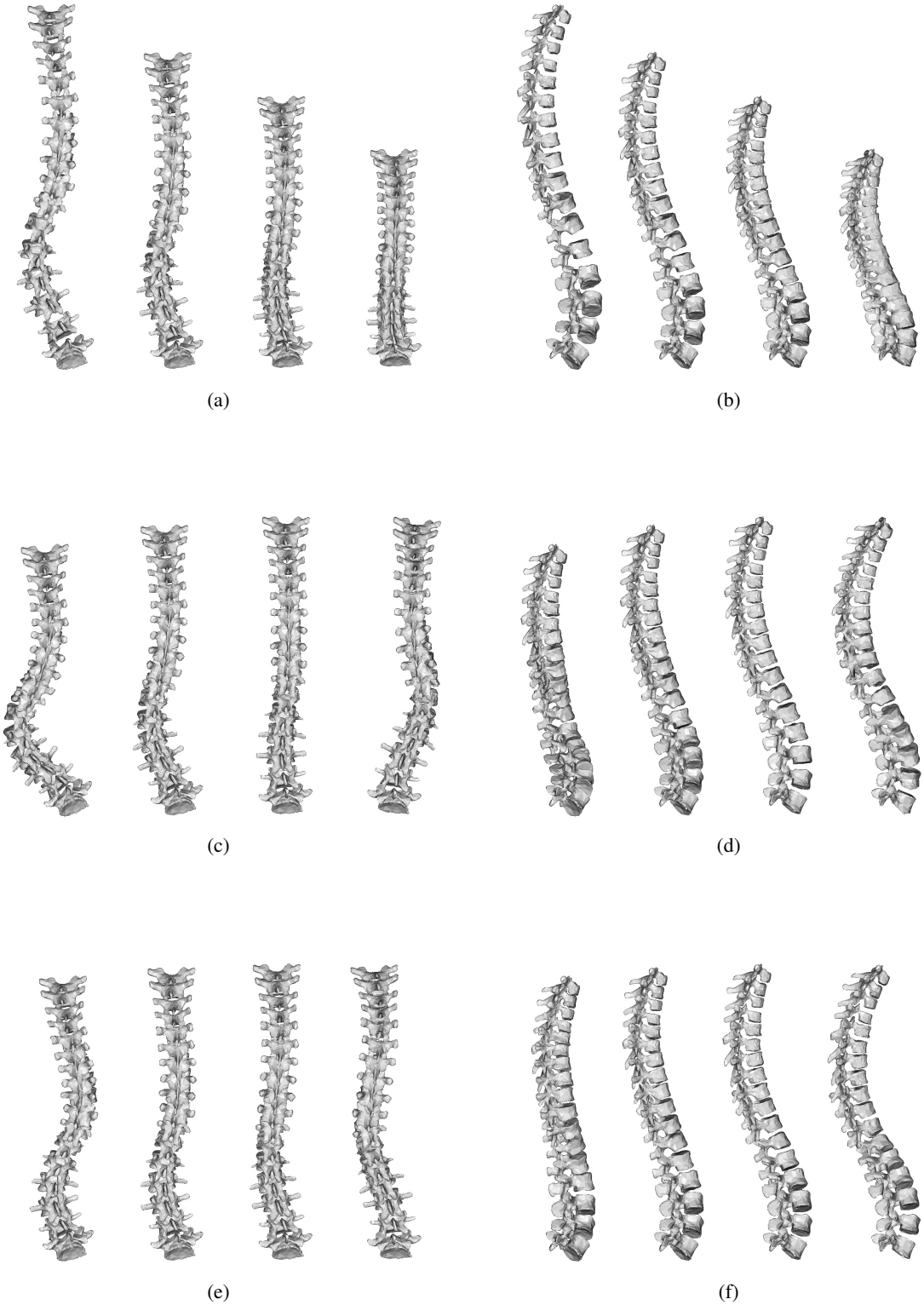

Figure 9: First, second and third principal deformation modes of AIS patient with type V curves. Posterior-anterior view (a) and lateral view (b) of the first principal deformation mode. Posterior-anterior view (c) and lateral view (d) of the second principal deformation mode. Posterior-anterior view (e) and lateral view (f) of the third principal deformation mode. Spine models were rendered for -3, -1, 1 and 3 times the standard deviation explained by the corresponding deformation mode.

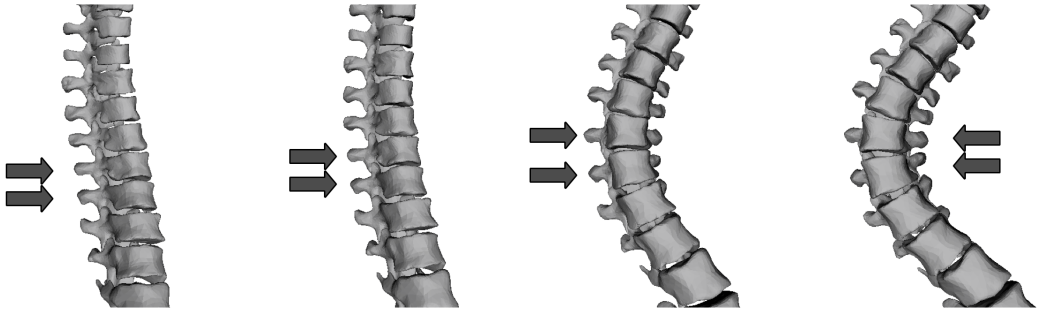

(a) (b) (c) (d)

Figure 10: Asymmetrical deformation of a vertebral body located near the apex of a spinal curve (a phenomena also called vertebra wedging) observe in the third principal deformation modes of a group of scoliotic patients which had 14 anatomical landmarks reconstructed on each of their vertebrae. Model reconstructions (with a fixed camera) for $-3\sqrt{\lambda_3}$ (a), $-\sqrt{\lambda_3}$ (b), $\sqrt{\lambda_3}$ (c) and $3\sqrt{\lambda_3}$ (d)

tended deformation mode in a given category of a surgical classification system (main thoracic for curves of the first type and thoracolumbar/lumbar for curves of the fifth type). It is also interesting to note that other important 3D curve patterns could also be identified. Those minor patterns would most probably be missed by a direct examination of the 3D spine models, which demonstrates the usefulness of the method to analyze rapidly and efficiently large databases of articulated models.

4.3 Combined Spine Shape and Local Vertebrae Shape Analysis

Surgical classifications of the spine are more concerned with the shape of the whole spine and less with the shape of individual vertebrae. This small interest is due to the fact that little can be done to correct vertebral deformations, especially if the patient's growth is over. However, there are several applications where a combined analysis of both spine and vertebrae shapes is very important.

First of all, image-guided spine surgeries are based on efficient and reliable registration methods. Those methods optimize a similarity measure between a spine model and spine images by deforming the spine model. Thus, registration methods would benefit from the correlation that exists between spine and vertebrae deformations. Moreover, vertebral deformations and spinal deformations in AIS patients are probably physiologically linked [30]. Thus analyzing vertebral deformations in the context of their underlying spinal deformation will lead to a better understanding of scoliosis progression.

Vertebrae shapes were already studied on dry human specimens [24], their deformation patterns were documented on scoliotic chickens [6] and asymmetric vertebral growth was experimented on rats [30]. However, our method offers the possibility of analyzing real patients and to visualize the relationships between the spinal deformities and vertebral deformities.

For this experiment 117 patients were selected and 14 anatomical landmarks for each vertebrae were digitized from the patients' radiographs. The principal deformation modes were then extracted using both the inter-vertebral transformations and the anatomical landmarks. Figure 10 illustrates that large deformations of the spine can be connected with vertebral deformations. In this particular case, the development of a thoracic curve (the camera does not move) is associated with an asymmetrical deformation of the vertebral bodies near the curve apex.

Although, vertebral deformations appears to be connected with spinal deformations our method cannot conclude if there is a causality link (or what this link is). The relationships observed between spinal curves types and vertebral deformations could however be used to validate conclusions obtained from animal studies or from biomechanical simulations.

5 Conclusion

A method to extract the principal modes of deformation from articulated models was described. The method consists in performing a principal component analysis in the tangent space of a Riemannian manifold. This manifold is composed of rigid transformations that describe the spine shape and also includes anatomical landmarks. We applied this method to databases of scoliotic patients reconstructed in 3D using biplanar radiographs.

Results suggest that PCA applied to a suitable representation of the spine, namely a set of rigid transformations, leads to an algorithm that can expose natural modes of deformation of the spine. Clinically relevant patterns of deformations were extracted and dimensionality reduction was successfully achieved. Patterns defined in existing surgical classifications were automatically identified from an unclassified group of scoliotic patients. The relationships that exists between clinically used 2D classifications and principal deformations modes were also assess qualitatively. Quantitative analysis will be performed in the future to demonstrate the qualities of the proposed method to the medical community.

Moreover, the application of the proposed method in the context of 3D classification of the scoliotic deformations was demonstrated by comparing the principal deformation modes of two groups of the Lenke classification. This experiment lead to the identification of deformations patterns that would have been very difficult to identify using another approach. An analysis of different patterns extracted from all Lenke's classes using the proposed method would thus be interesting to realize in the future.

One important characteristic of the proposed method behind these promising results is the absence an arbitrary selection of clinical indices. All the information needed to describe the 3D spine models is used, but it is regrouped into uncorrelated modes and sorted in descending order of explained variance. The proposed method is therefore a promising analytical tool and it will certainly contribute to the definition of new 3D classifications.

We also showed that the vertebral deformations could be linked to the deformation of the whole spine. This experiment is compatible with the "vicious cycle" described by Stokes et al. [30] that could explain a progression mechanism of scoliosis. However, describing vertebrae shapes with anatomical landmarks might be simplistic and alternate representation such as spherical harmonics or medial axis representations could also be used.

A very promising perspective is the longitudinal analysis of patients. Multiple acquisition of the patients' spine geometry could be used to extract progression modes instead of deformation modes. This could be a significant breakthrough since patients belonging to more severe progression modes could be followed more closely by their physician and patients with lower progression risks could be treated less aggressively.

Finally, one of the reasons to perform dimensionality reduction on statistical shape models is to reduce the number of DOF that needs to be optimized during model registration. The proposed method will therefore be integrated to a spine registration algorithm in the future. It might also be useful for the integration of a large number of rigid structures in non-rigid registration procedures [19] of the whole human torso.

Acknowledgement

This work was funded by the Natural Sciences and Engineering Research Council (NSERC) of Canada, the Québec's Technology and Nature Research Funds (Fonds de Recherche sur la Nature et les Technologies de Québec) and the Canadian Institutes of Health Research (CIHR).

References

[1] S. Al-Zubi and G. Sommer. Learning deformations of human arm movement to adapt to environmental constraints. *Articulated Motion and Deformable Objects. 4th International Conference, AMDO 2006. Proceedings (Lecture Notes in Computer Science Vol.4069)*, pages 203 – 12, 2006.

[2] C.-E. Aubin, J. Dansereau, F. Parent, H. Labelle, and J.A. de Guise. Morphometric evaluations of personalised 3d reconstructions and geometric models of the human spine. *Med. Bio. Eng. Comp.*, 35(6):611–618, 1997.

[3] S. Benameur, M. Mignotte, S. Parent, H. Labelle, W. Skalli, and J. de Guise. 3D/2D registration and segmentation of scoliotic vertebrae using statistical models. *Computerized Medical Imaging and Graphics*, 27(5):321–37, 2003.

[4] Charles Bergeron, Farida Cheriet, Janet Ronsky, Ronald Zernicke, and Hubert Labelle. Prediction of anterior scoliotic spinal curve from trunk surface using support vector regression. *Engineering Applications of Artificial Intelligence*, 18(8):973 – 82, 2005.

[5] Jonathan Boisvert, Xavier Pennec, Nicholas Ayache, Hubert Labelle, and Farida Cheriet. 3D anatomical variability assessment of the scoliotic spine using statistics on Lie groups. In *Proc. 2006 IEEE International Symposium on Biomedical Imaging*, pages 750–753, 2006.

[6] C. Coillard and C. H. Rivard. Vertebral deformities and scoliosis. *Eur. Spine J.*, 5:91–100, 1996.

[7] Jonathan Deutscher and Ian Reid. Articulated body motion capture by stochastic search. *International Journal of Computer Vision*, 61(2):185 – 205, 2005.

[8] Luc Duong, Farida Cheriet, and Hubert Labelle. Three-dimensional classification of spinal deformities using fuzzy clustering. *Spine*, 31:923–923, Apr 2006.

[9] P. T. Fletcher, Conglin Lu, S. M. Pizer, and Sarang Joshi. Principal geodesic analysis for the study of nonlinear statistics of shape. *IEEE Trans. Med. Imaging*, 23(8), 2004.

[10] M. Fleute, S. Lavallee, and L. Desbat. Integrated approach for matching statistical shape models with intra-operative 2D and 3D data. In *Proceedings of MICCAI*, 2002.

[11] Herbert Goldstein. *Classical Mechanics*, pages 164–166. Addison-Wesley, 1980.

[12] J. Gonzalez, J. Varona, F.X. Roca, and J.J. Villanueva. Analysis of human walking based on aspaces. *Proc. of Articulated Motion and Deformable Objects*, pages 177 – 88, 2004.

[13] R.D. Green and Ling Guan. Quantifying and recognizing human movement patterns from monocular video images-part ii: applications to biometrics. *IEEE Trans. Circuits Syst. Video Technol. (USA)*, 14(2):191 – 8, 2004.

[14] Richard D. Green and Ling Guan. Quantifying and recognizing human movement patterns from monocular video images - part i: A new framework for modeling human motion. *IEEE Transactions on Circuits and Systems for Video Technology*, 14(2):179 – 190, 2004.

[15] Xianhua Jiang and Yuichi Motai. Learning by observation of robotic tasks using on-line pca-based eigen behavior. *Proc. International Symposium on Computational Intelligence in Robotics and Automation*, pages 391–6, 2005.

[16] H. A. King. Selection of fusion levels for posterior instrumentation and fusion in idiopathic scoliosis. *Orthop Clin North Am*, 19:247–255, Apr 1988.

[17] L. G. Lenke, R. R. Betz, K. H. Bridwell, D. H. Clements, J. Harms, T. G. Lowe, and H. L. Shufflebarger. Intraobserver and interobserver reliability of the classification of thoracic adolescent idiopathic scoliosis. *J. Bone Joint Surg. Am.*, 80:1097–1106, Aug 1998.

[18] L. G. Lenke, R. R. Betz, J. Harms, K. H. Bridwell, D. H. Clements, T. G. Lowe, and K. Blanke. Adolescent idiopathic scoliosis: a new classification to determine extent of spinal arthrodesis. *J. Bone Joint Surg. Am.*, 83-A:1169–1181, Aug 2001.

[19] J. A. Little, D. L. G. Hill, and D. J. Hawkes. Deformations incorporating rigid structures. *Computer Vision and Image Understanding*, 66(2):223–32, May 1997.

[20] C. Lorenz and N. Krahnstover. Generation of point-based 3d statistical shape models for anatomical objects. *Comput. Vis. Image Underst.*, 77(2):175 – 91, 2000.

[21] Alberto Negrini and Stefano Negrini. The three-dimensional easy morphological (3-DEMO) classification of scoliosis, part II: repeatability. *Scoliosis*, 1:23, Dec 2006.

[22] Stefano Negrini and Alberto Negrini. The three-dimensional easy morphological (3-DEMO) classification of scoliosis - part III, correlation with clinical classification and parameters. *Scoliosis*, 2:5, Mar 2007.

[23] Stefano Negrini, Alberto Negrini, Salvatore Atanasio, and Giorgio C. Santambrogio. Three-dimensional easy morphological (3-DEMO) classification of scoliosis, part I. *Scoliosis*, 1:20, Dec 2006.

[24] Stefan Parent, Hubert Labelle, Wafa Skalli, Bruce Latimer, and Jacques de Guise. Morphometric analysis of anatomic scoliotic specimens. *Spine*, 27:2305–2311, Nov 2002.

[25] X. Pennec. Computing the mean of geometric features - application to the mean rotation. Research Report RR-3371, INRIA, March 1998.

[26] Xavier Pennec. Intrinsic statistics on Riemannian manifolds: Basic tools for geometric measurements. *Journal of Mathematical Imaging and Vision*, 25(1):127–154, 2006.

[27] P. Poncet, J. Dansereau, and H. Labelle. Geometric torsion in idiopathic scoliosis: three-dimensional analysis and proposal for a new classification. *Spine*, 26:2235–2243, Oct 2001.

[28] C. Sminchisescu and B. Triggs. Estimating articulated human motion with covariance scaled sampling. *Int. J. Robot. Res. (USA)*, 22(6):371 – 91, 2003.

[29] I. A. Stokes. Three-dimensional terminology of spinal deformity. a report presented to the scoliosis research society by the scoliosis research society working group on 3-D terminology of spinal deformity. *Spine*, 19:236–248, Jan 1994.

[30] I. A. Stokes, H. Spence, D. D. Aronsson, and N. Kilmer. Mechanical modulation of vertebral body growth. implications for scoliosisprogression. *Spine*, 21:1162–1167, May 1996.

[31] Ian A. F. Stokes and David D. Aronsson. Identifying sources of variability in scoliosis classification using a rule-based automated algorithm. *Spine*, 27:2801–2805, Dec 2002.

[32] Y. Yacoob and M.J. Black. Parameterized modeling and recognition of activities. *Comput. Vis. Image Underst. (USA)*, 73(2):232 – 47, 1999.

[33] Zhou Ziheng, Adam Prugel-Bennett, and Robert I. Damper. A bayesian framework for extracting human gait using strong prior knowledge. *IEEE Transactions on Pattern Analysis and Machine Intelligence*, 28(11):1738 – 1752, 2006.